Frequency-domain multiscale quantum mechanics/electromagnetics simulation method

Lingyi Meng, Zhenyu Yin, ChiYung Yam, SiuKong Koo, Quan Chen, Ngai Wong, and GuanHua Chen

Articles you may be interested in

A multi-scale modeling of junctionless field-effect transistors
Applied Physics Letters 103, 062109 (2013); 10.1063/1.4817911

Time-dependent density functional theory quantum transport simulation in non-orthogonal basis
The Journal of Chemical Physics 139, 224111 (2013); 10.1063/1.4840655

Dissipative time-dependent quantum transport theory
The Journal of Chemical Physics 138, 164121 (2013); 10.1063/1.4802592

Time-dependent density functional theory for open systems with a positivity-preserving decomposition scheme for environment spectral functions
The Journal of Chemical Physics 142, 144112 (2015); 10.1063/1.4917172

Dissipative time-dependent quantum transport theory: Quantum interference and phonon induced decoherence dynamics
The Journal of Chemical Physics 142, 164101 (2015); 10.1063/1.4918771

Time-dependent quantum transport: An efficient method based on Liouville-von-Neumann equation for single-electron density matrix
The Journal of Chemical Physics 137, 044113 (2012); 10.1063/1.4737864
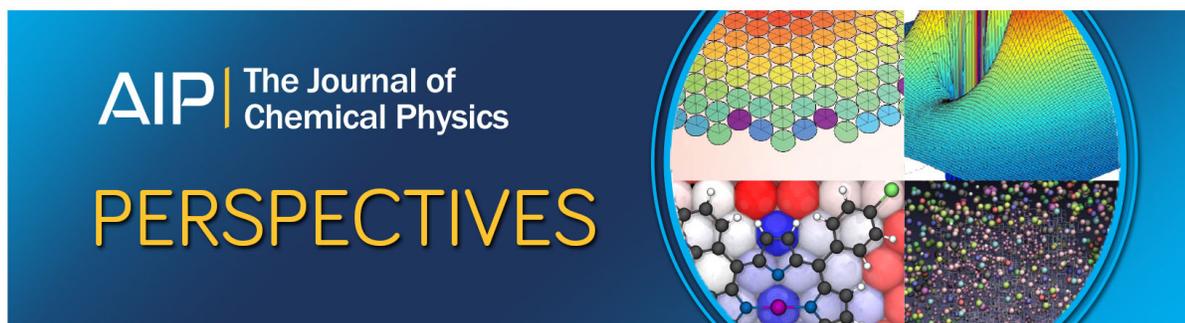
Frequency-domain multiscale quantum mechanics/electromagnetics simulation method

Lingyi Meng,[1] Zhenyu Yin,[1] ChiYung Yam,[1,a] SiuKong Koo,[1] Quan Chen,[2] Ngai Wong,[2] and GuanHua Chen[1,a]

[1]*Department of Chemistry, The University of Hong Kong, Pokfulam Road, Hong Kong*
[2]*Department of Electrical and Electronic Engineering, The University of Hong Kong, Pokfulam Road, Hong Kong*

A frequency-domain quantum mechanics and electromagnetics (QM/EM) method is developed. Compared with the time-domain QM/EM method [Meng *et al.*, J. Chem. Theory Comput. **8**, 1190–1199 (2012)], the newly developed frequency-domain QM/EM method could effectively capture the dynamic properties of electronic devices over a broader range of operating frequencies. The system is divided into QM and EM regions and solved in a self-consistent manner via updating the boundary conditions at the QM and EM interface. The calculated potential distributions and current densities at the interface are taken as the boundary conditions for the QM and EM calculations, respectively, which facilitate the information exchange between the QM and EM calculations and ensure that the potential, charge, and current distributions are continuous across the QM/EM interface. Via Fourier transformation, the dynamic admittance calculated from the time-domain and frequency-domain QM/EM methods is compared for a carbon nanotube based molecular device. © *2013 AIP Publishing LLC*. [http://dx.doi.org/10.1063/1.4853635]

I. INTRODUCTION

With the continuous miniaturization trend, the feature size of transistors is expected to reach close to 10 nm in a few years. In the meantime, operation frequencies increase towards terahertz. Quantum effects, atomistic details as well as propagation of electromagnetic waves should be taken into account in modeling and designing emerging electronic devices.[1–3] The interaction between charge and electromagnetic field plays an essential role in many other novel devices and materials such as transistors,[3,4] photovoltaic devices,[5–8] and metamaterials.[9,10] By balancing the accuracy and efficiency, a hybrid method which combines quantum mechanics (QM) and electromagnetics (EM), the QM/EM method,[1,2] has been developed.

In the QM/EM method, the active device regions are modeled via the atomistic QM method while the interconnects and substrates are modeled classically by solving Maxwell's equations via the computational EM solvers. Having been successfully implemented for static[1,3] and time-dependent fields,[2] the QM/EM method is extended to the frequency-domain in this work. The frequency-dependent bias voltage is treated as a perturbation. Compared to the time-domain QM/EM method, the frequency-domain QM/EM method is expected to be particularly efficient in the low frequency regime as long simulation time is required in the time-domain method to capture low frequency characteristics.

An alternating current (AC) quantum transport theory was developed recently to ensure both gauge-invariance and current-continuity.[11] The induced potential distribution due to an external applied voltage is considered and obtained self-consistently by solving the Poisson equation with proper boundary conditions. The time-dependent density-functional theory (TDDFT)[12] has been exploited in this AC quantum transport theory to investigate the dynamic properties of molecular devices. For practical purpose, the wide band limit (WBL) approximation is adopted[13,14] to describe the electrodes and this has also been applied to study graphene nanoribbon and carbon nanotube based molecular devices.[15]

By Fourier transformation of the time-domain equations in the EM solver, the coupled frequency-dependent EM and drift-diffusion equations can be solved to model electronic devices, interconnects, substrates, and dielectrics.[16–20] Based on the finite volume method (FVM),[21] the potential formalism of Maxwell's equations and a mimetic discretization of differential operators are adopted to guarantee local charge conservation. Instead of the electric field $\vec{E}$ and the magnetic field $\vec{H}$, the scalar potential V and vector potential $\vec{A}$ are chosen as basic variables which facilitate the interface with conventional engineering solvers and the QM method.[2] The EM solver based on the potential formulation has been validated for a number of cases in which the simulation results were compared with measured data on test structures developed in industry.[22,23] The solver has been transferred into a series of commercial tools of MAGWEL.[24] One can achieve the simplicity of the frequency-domain solver by assuming the system being excited by a sinusoidal perturbation with small amplitude (the small-signal assumption), which results in a pure time-harmonic solution.[25]

Theoretical models at different scales (e.g., first-principles methods and classical simulation methods) could

a)Authors to whom correspondence should be addressed. Electronic addresses: yamcy@yangtze.hku.hk and ghc@everest.hku.hk

be integrated in "decoupled" or "coupled" schemes. Key parameters of the electronic systems are extracted from the QM simulation and embedded in the EM simulation. Our QM/EM method adopts a coupled integration scheme: The potential V at the QM and EM interface calculated by the EM solver is used as the boundary condition for the QM calculation. In return, the current density distribution at the interface resulted from the QM calculation is used as a part of the boundary condition for the EM solution.

II. METHODOLOGIES

A. Electromagnetics simulation

The differential forms for the Maxwell's equations are listed as[26,27]

$$\nabla \cdot \vec{D} = \rho, \tag{1}$$

$$\nabla \cdot \vec{B} = 0, \tag{2}$$

$$\nabla \times \vec{E} = -\frac{\partial}{\partial t}\vec{B}, \tag{3}$$

$$\nabla \times \vec{H} = \vec{J} + \frac{\partial}{\partial t}\vec{D}, \tag{4}$$

where $\vec{D}$, $\vec{E}$, $\vec{B}$, and $\vec{H}$ denote the electrical induction, the electric field, the magnetic induction, and the magnetic field, respectively. And ρ and $\vec{J}$ denote the charge and current densities, respectively.

The following constitutive relations are employed to relate the inductances $\vec{D}$ and $\vec{B}$ to the field strengths $\vec{E}$ and $\vec{H}$:

$$\vec{D} = \varepsilon\vec{E}, \tag{5}$$

$$\vec{B} = \mu\vec{H}, \tag{6}$$

where ϵ and μ are the material permittivity and permeability, respectively. In the following simulations, we assume the structure is nonmagnetic, i.e., $\mu = \mu_0$.[22,23]

In lieu of the original Maxwell's equations that use vector field $\vec{E}$ and $\vec{H}$ as basic variables, an alternative version of the Maxwell's equations based on potentials (the scalar potential V and vector potential $\vec{A}$) could be derived by employing the transform relations

$$\vec{B} = \nabla \times \vec{A}, \tag{7}$$

$$\vec{E} = -\nabla V - \frac{\partial}{\partial t}\vec{A}. \tag{8}$$

Combined with Eqs. (7) and (8), Eqs. (1) and (4) are rewritten as

$$\nabla \cdot \left[\varepsilon\left(-\nabla V - \frac{\partial}{\partial t}\vec{A}\right)\right] - \rho = 0, \tag{9}$$

$$\nabla \times \left[\frac{1}{\mu}(\nabla \times \vec{A})\right] - \left[\vec{J} + \frac{\partial}{\partial t}\left(\varepsilon\left(-\nabla V - \frac{\partial}{\partial t}\vec{A}\right)\right)\right] = 0. \tag{10}$$

An additional constraint (or gauge condition) is necessary to uniquely determine potentials $\vec{A}$ and V for any given $\vec{E}$

and $\vec{B}$. Two commonly used gauges are Coulomb gauge and Lorentz gauge.[26] Without loss of generality, Lorentz gauge is employed throughout the numerical simulations as

$$\nabla \cdot \vec{A} + \mu\varepsilon\frac{\partial}{\partial t}V = 0. \tag{11}$$

The frequency-domain Maxwell's equations can then be obtained by replacing all time differentials with $i\omega$:

$$\vec{E} = -\nabla V - i\omega\vec{A}, \tag{12}$$

$$\nabla \cdot [\varepsilon(-\nabla V - i\omega\vec{A})] - \rho = 0, \tag{13}$$

$$\nabla \times \left[\frac{1}{\mu}(\nabla \times \vec{A})\right] - [\vec{J} + i\omega(\varepsilon(-\nabla V - i\omega\vec{A}))] = 0, \tag{14}$$

$$\nabla \cdot \vec{A} + i\omega\mu\varepsilon V = 0, \tag{15}$$

where ω is the frequency. Therefore, Eqs. (7) and (12)–(15) form together the governing equations for solving the electromagnetic waves in the frequency-domain. Finally, all solved field or potential quantities are the phasor equivalents of the corresponding time-domain solutions.

In Eq. (14), the operator $\nabla \times (\nabla \times)$ is intrinsically singular. To recover a Laplacian-like operator and thus eliminate the singularity, Eq. (14) is subtracted by the divergence of the gauge condition Eq. (15), which yields

$$\nabla \times (\nabla \times \vec{A}) - \nabla(\nabla \cdot \vec{A}) + Ki\omega\varepsilon(\nabla V + i\omega\vec{A})$$
$$- K\nabla(\varepsilon i\omega V) - K\vec{J} = 0. \tag{16}$$

The dimensionless constant $K = (1/c^2)(\lambda/\tau)^2$, where c is the speed of light in vacuum, and λ and τ denote the scaling parameters for lengths and time, respectively.[23]

The dependency of the current $\vec{J}$ on the electric field and the free carrier densities is determined by the medium under consideration in the EM region. For the conductors in the system, the current $\vec{J}$ is given by classical Ohm's law,

$$\vec{J} = \sigma\vec{E} = \sigma(-\nabla V - i\omega\vec{A}), \tag{17}$$

where σ is the conductivity of the conductor. The current density satisfies the current continuity equation and no free charge densities need to be solved inside the conductor,

$$\nabla \cdot \vec{J} + i\omega\rho = 0. \tag{18}$$

In dielectrics, there are also no free charges and the dielectric losses are neglected. Therefore, no current equation needs to be solved in insulators.[22,23]

For the semiconductors, the current due to electrons (or holes) is split into drift and diffusion terms

$$\vec{J}_n = q\mu_n n\vec{E} + k_B T\mu_n\nabla n$$
$$= q\mu_n n(-\nabla V - i\omega\vec{A}) + k_B T\mu_n\nabla n, \tag{19a}$$

$$\vec{J}_p = q\mu_p p\vec{E} - k_B T\mu_p\nabla p$$
$$= q\mu_p p(-\nabla V - i\omega\vec{A}) - k_B T\mu_p\nabla p, \tag{19b}$$

where n and p correspond to the electron and hole densities, respectively. $\mu_{n(p)}$ is the mobility of the electron(hole). k_B

denotes the Boltzmann constant and T the temperature. The continuity equations for the electrons and holes are

$$\nabla \cdot \vec{J}_n - qi\omega n - qR(n, p) = 0, \qquad (20a)$$

$$\nabla \cdot \vec{J}_p + qi\omega p + qR(n, p) = 0, \qquad (20b)$$

where R is the charge carrier generation rate. Finally, the total charge density in semiconductors is given as

$$\rho = q(p - n + N_D - N_A), \qquad (21)$$

where N_D and N_A are the donor and acceptor concentrations due to the doping, respectively.

Any independent variable X in the frequency-domain is comprised of a static (or DC) component and a frequency-domain response (or AC) component:

$$X = X^{DC} + X^{AC} \exp(i\omega t), \qquad (22)$$

where X could be $V, n, p, \vec{A}$. In the frequency-domain method, the AC signal ($V^{AC}, n^{AC}, p^{AC}, \vec{A}^{AC}$) is solved as a perturbation of the static solution ($V^{DC}, n^{DC}, p^{DC}, \vec{A}^{DC}$).

The local charge conservation can be satisfied by applying the spatial gridding scheme based on the FVM and adopting a mimetic discretization of differential operators.[22,23] The application of boundary conditions and interface conditions for the frequency-domain EM solver is similar to one for the time-domain simulations.[2] In the current implementation, the EM solvers are coded in MATLAB, and we assume that there is no charge generation or recombination, i.e., the net charge generation rate $R(n, p)$ in the current continuity equations is set to zero.[2]

B. Quantum mechanical simulation

Unlike electromagnetic simulations which treat systems as continuous media, quantum mechanical simulations have abilities to capture features of electrons in atomic scale at the cost of high computational time. During last few years, many efforts have been devoted into the area of time-dependent quantum transport in open systems.[13,14,28–31] Based on the Keldysh non-equilibrium Green's function (NEGF)[32] formalism, the current through electrode α can be expressed as

$$I_\alpha(t) = \frac{e}{h} \int dt_1 Tr[G^<(t, t_1)\Sigma_\alpha^a(t_1, t)$$
$$+ G^r(t, t_1)\Sigma_\alpha^<(t_1, t) + C.C.], \qquad (23)$$

where G^γ and Σ^γ are the Green's functions and self-energies, respectively, and $\gamma = r, a, <$. The system couples to the lead α via the self-energy Σ_α and Eq. (23) gives the real-time current at lead α. Through a double-time Fourier transform, Eq. (23) is converted into the frequency-domain, and the frequency-dependent current is given by

$$I_\alpha(\omega) = \frac{e}{\hbar} \iint \frac{dE}{2\pi} \frac{dE_1}{2\pi} Tr[G^r(E + \hbar\omega, E_1)\Sigma_\alpha^<(E_1, E)$$
$$+ G^<(E + \hbar\omega, E_1)\Sigma_\alpha^a(E_1, E)$$
$$- \Sigma_\alpha^<(E + \hbar\omega, E_1)G^a(E_1, E)$$
$$- \Sigma_\alpha^r(E + \hbar\omega, E_1)G^<(E_1, E)], \qquad (24)$$

where the double-time Fourier transform is defined as

$$F(E_1, E_2) = \int f(t_1, t_2) \exp(E_1 t_1 - E_2 t_2) dt_1 t_2, \qquad (25)$$

In practice, we assume the applied bias is small enough to be treated as a perturbation. Thus, a first order approximation[33] is applied

$$G^\gamma(E_1, E_2) = G_0^\gamma(E_1, E_2)\delta(E_1 - E_2) + \delta G^\gamma(E_1, E_2)$$
$$\Sigma^\gamma(E_1, E_2) = \Sigma_0^\gamma(E_1, E_2)\delta(E_1 - E_2) + \delta\Sigma^\gamma(E_1, E_2), \qquad (26)$$

where G_0 and Σ_0 are ground state Green's function and self-energy when no AC bias voltage is applied. Within the WBL approximation, the AC current in the frequency-domain is given by

$$I_\alpha(\omega) = \frac{e^2}{h} \int \frac{dE}{\omega}(f - f^+)Tr\big[-iG_0^a\Gamma_\alpha G_0^{r,+} v_\alpha$$
$$+ G_0^a\Gamma_\alpha G_0^{r,+}\Gamma_\beta(v_\alpha - v_\beta)\big]$$
$$+ \frac{e}{h} \int dE(f - f^+)Tr\big[iV(\omega)G_0^a\Gamma_\alpha G_0^{r,+}\big], \qquad (27)$$

where α, β are indices of lead, and f is the Fermi distribution function. For simplicity, f, f^+, and $G^{r,+}$ represent $f(E)$, $f(E + \hbar\omega)$, and $G^r(E + \hbar\omega)$, respectively. v_α is the AC bias on lead α and $V(\omega)$ gives the frequency dependent potential distribution inside the device, projected on the atomic basis. Compared to previous work,[34,35] the real space self-consistent potential distribution[11,36] $V(\vec{r}, \omega)$ is included explicitly by solving the Poisson equation to ensure gauge invariance,

$$\nabla^2 V(\vec{r}, \omega) = \rho(\vec{r}, \omega), \qquad (28)$$

where ρ is the charge density in the device part under an AC bias, and can be expressed with the corresponding electron density matrix $\sigma_{\mu\nu}$ as

$$\rho(\vec{r}) = \sum_{\mu\nu} \sigma_{\mu\nu}\phi_\mu(\vec{r})\phi_\nu(\vec{r}), \qquad (29)$$

where $\phi(\vec{r})$ is the electron basis function. In our implementation, the induced electron density matrix is obtained from the first order lesser Green's function via

$$\delta\hat{\sigma} = \frac{ie}{h} \int \frac{dE}{2\pi} \delta G^<(E + \hbar\omega, E), \qquad (30)$$

$$\delta G^<(E + \hbar\omega, E) = G_0^r(E + \hbar\omega)\delta\Sigma_0^<(E + \hbar\omega, E)G_0^a(E)$$
$$+ G_0^r(E + \hbar\omega)V(\omega)G_0^<(E)$$
$$+ G_0^<(E + \hbar\omega)V(\omega)G_0^a(E). \qquad (31)$$

Equations (28)–(31) are solved in a self-consistent fashion and the current flowing through the electronic device can be evaluated using Eq. (27). It is noted that the current evaluated from Eqs. (23), (24), and (27) is particle current. In cases of charge depletion or accumulation within the electronic device, displacement current should be considered to ensure current conservation. This can be obtained readily from the rate of change of electric field.

C. Boundary condition at QM/EM interface

In the frequency-domain QM/EM simulations, the coupled QM and EM solvers are integrated together. Similar to the time-domain QM/EM method, potential distribution and current density are used as boundary conditions in QM and EM solvers for information exchange. Initially, the scalar potential distribution is calculated by the EM solver for the whole system including the QM region. The complex potential V at the QM and EM interface is used as the boundary condition for the QM solver. Then the complex current density at the interface calculated from the QM method is fed back to the EM solver as the boundary condition. The whole process is iterated until the potential distribution and current density converge. In the current implementation, due to the simplicity of the systems, convergence is readily achieved within few cycles. Depending on the complexity of the systems, more sophisticated convergence acceleration techniques are required, for instance, Broyden's mixing.[37]

To realize the seamless coupling between the EM and QM solvers, the following equations for the scalar and vector potentials in the QM region should be solved[2]

$$\nabla \cdot [\vec{J}_{QM} + i\omega\varepsilon(\nabla V + i\omega\vec{A})] = 0, \tag{32}$$

$$\nabla \times (\nabla \times \vec{A}) - \nabla(\nabla \cdot \vec{A}) + Ki\omega\varepsilon(\nabla V + i\omega\vec{A})$$
$$- K\nabla(i\omega\varepsilon V) - K\vec{J}_{QM} = 0, \tag{33}$$

where the particle current density $\vec{J}_{QM}$ is calculated by the QM method. The displacement current is defined by the term $i\omega\varepsilon(\nabla V + i\omega\vec{A})$ in Eq. (32), and the total current should be conserved through the entire system.

III. RESULTS AND DISCUSSIONS

The frequency-domain QM/EM method has been applied to a carbon nanotube (CNT) electronic device. Figure 1 shows the cross-section of the three-dimensional device. The system comprises of a (5, 5) CNT connected to two aluminum elec-

trodes embedded in a silicon substrate. The entire structure has a dimension of $8 \times 5 \times 5$ nm³: CNT and part of electrodes (totally 128 aluminum atoms and 60 carbon atoms) are included in the QM region with the size of $4 \times 1 \times 1$ nm³ and the rest of the system is included in the EM region. The QM region contains full atomistic details while the continuum model is used in the EM region. In the EM region, the conductivity of aluminum electrodes is set as 3.37×10^7 S/m,[2] and an undoped silicon substrate with a relative permittivity of 11.9 is used.[2] The FVM discretization generates $15 \times 11 \times 11$ nodes and 4994 links.

To simulate dynamic properties, the steady state of the system is first obtained by grounding both contacts 1 and 2. AC bias voltages at different frequencies with amplitude of 0.1 mV are then applied on the electrodes. To increase the efficiency, the density-functional tight-binding (DFTB)[38] Hamiltonian is adopted in Eq. (27) to simulate AC quantum transport in the QM region. In the simulations, the total current and the particle current across the surface S in Fig. 1 are evaluated and analyzed. To verify our frequency-domain QM/EM method, time-domain QM/EM[2] calculations are performed which sinusoidal transient bias voltages with different amplitudes (0.1 mV, 0.01 V, and 1.0 V) and period of 5 fs are applied at $t = 0$ to the same system. The simulation results are then Fourier transformed to the frequency-domain for comparison.[15] It is noted that the particle current flowing through the substrate is insignificantly small since the substrate is built from undoped silicon. Therefore, the particle current across S essentially equals to the particle current (I_{QM}) flowing through the QM region.

Figure 2 plots the dynamic admittance $G(\omega) = I(\omega)/V(\omega)$ for the particle current. Our frequency-domain QM/EM is a linear response theory with respect to the bias voltage. As long as the applied voltage is small enough, the results from the time-domain and frequency-domain simulations agree well over frequencies up to 0.6 eV ($\sim$140 THz) which validates the frequency-domain QM/EM method. At a high AC bias voltage (1.0 V), where the system is far from equilibrium, it is shown that the dynamic admittance obtained from time-domain simulation results deviates from that obtained at low AC bias voltages (0.1 mV and 0.01 V) due to the nonlinear effect. It is also observed that the deviation becomes more
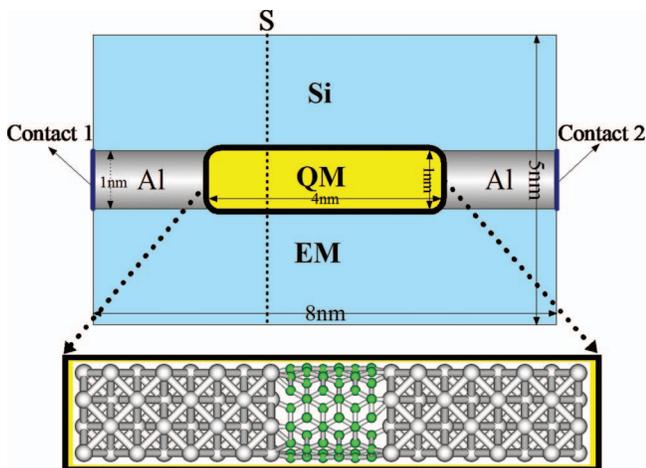

FIG. 1. Schematic diagram to illustrate the dynamic multiscale QM/EM approach. Region enclosed in the central box is simulated by quantum mechanics with full atomistic details while the outer EM region is simulated by the EM method.
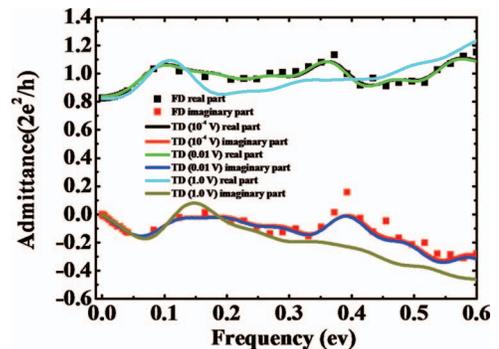

FIG. 2. The comparison of the dynamic admittance for the particle currents calculated by the time-domain (with the bias voltage of 0.1 mV, 0.01 V, and 1.0 V, respectively) (TD) and frequency-domain (FD) QM/EM simulation methods at different operating frequencies.
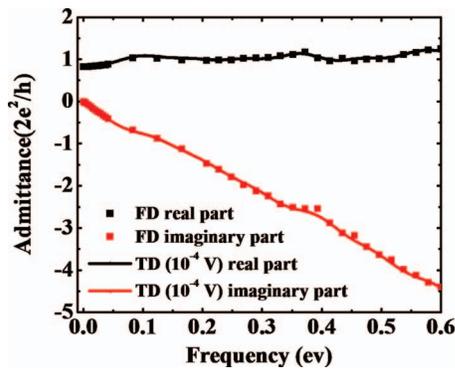
FIG. 3. The comparison of the dynamic admittance for the total currents calculated by the time-domain (with the bias voltage of 0.1 mV) (TD) and frequency-domain (FD) QM/EM simulation methods at different operating frequencies.

good agreement. Compared with the time-domain counterpart, the frequency-domain QM/EM method is found to be more efficient in the low frequency regime, in particular, in the operating frequencies of electronic devices, and is thus an important modeling method for emerging electronic devices. While it has been employed to simulate the electronic devices so far, the QM/EM method can be used to study the plasmonic effects such as plasmon enhanced optical phenomena.

prominent at higher frequencies. Being a linear response theory, the dynamic admittance, however, remains the same in the frequency domain calculations for both high and low AC bias voltages. This shows that our method is valid at the low AC bias voltage and low frequency regime. To simulate nonlinear effect at the high bias voltage, a small-signal technique is commonly used where a DC bias voltage is applied to drive the system out of equilibrium and a small AC bias is applied as a perturbation around this bias point.

Figure 3 shows the dynamic admittance for the total current. In our simulations, the displacement current contributes only to the susceptance (the imaginary part of the admittance) since the applied voltage is a real number. From Fig. 3, the magnitude of the susceptance increases as the frequency increases which shows that the displacement current contributes a significant component to the total current at high frequencies.

The dynamic characteristics of electronic devices at low operating frequencies could be investigated efficiently by the frequency-domain QM/EM method. At low frequencies, the potential distributions and charge densities resemble that of the steady state, and the self-consistency is in general readily achieved. For instance, at frequencies lower than 10^{11} Hz (~1 meV), the self-consistent QM calculations [Eqs. (28)–(31)] converge within 20 cycles. In contrast, a resolution of 10^{11} Hz in the time-domain simulations requires propagation time of about 60 ps. Thus, the frequency-domain QM/EM method serves as an efficient alternative to the time-domain QM/EM method in the low frequency regime. However, at high frequencies, the time-domain QM/EM method is more effective, since a significant charge redistribution occurs in the electronic devices which requires more iterations to achieve a self-consistent frequency-domain QM/EM solution.

IV. SUMMARY

The family of our multiscale QM/EM simulation methods has been supplemented by the newly developed frequency-domain method. Through the application to a carbon nanotube molecular device, the time-domain and frequency-domain QM/EM methods are compared with the

[1]C. Yam, L. Meng, G. H. Chen, Q. Chen, and N. Wong, Phys. Chem. Chem. Phys. **13**, 14365–14369 (2011).
[2]L. Meng, C. Yam, S. Koo, Q. Chen, N. Wong, and G. H. Chen, J. Chem. Theory Comput. **8**, 1190–1199 (2012).
[3]C. Yam, J. Peng, Q. Chen, S. Markov, J. Z. Huang, N. Wong, W. C. Chew, and G. H. Chen, Appl. Phys. Lett. **103**, 062109 (2013).
[4]P.-F. Wang, X. Lin, L. Liu, Q.-Q. Sun, P. Zhou, X.-Y. Liu, W. Liu, Y. Gong, and D. W. Zhang, Science **341**, 640–643 (2013).
[5]J.-L. Brédas, J. E. Norton, J. Cornil, and V. Coropceanu, Acc. Chem. Res. **42**, 1691–1699 (2009).
[6]L. Meng, Y. Shang, Q. Li, Y. Li, X. Zhan, Z. Shuai, R. G. E. Kimber, and A. B. Walker, J. Phys. Chem. B **114**, 36–41 (2010).
[7]L. Meng, D. Wang, Q. Li, Y. Yi, J.-L. Bredas, and Z. Shuai, J. Chem. Phys. **134**, 124102 (2011).
[8]Y. Shang, Q. Li, L. Meng, D. Wang, and Z. Shuai, Appl. Phys. Lett. **97**, 143511 (2010).
[9]J. Li and C. T. Chan, Phys. Rev. B **72**, 195103 (2005).
[10]L. Zhou, W. Wen, C. T. Chan, and P. Sheng, Phys. Rev. Lett. **94**, 243905 (2005).
[11]J. Zhang, Z. Yin, X. Zheng, C. Yam, and G. H. Chen, Eur. Phys. J. B **86**, 423 (2013).
[12]E. Runge and E. K. U. Gross, Phys. Rev. Lett. **52**, 997–1000 (1984).
[13]X. Zheng, G. H. Chen, Y. Mo, S. Koo, H. Tian, C. Yam, and Y. Yan, J. Chem. Phys. **133**, 114101 (2010).
[14]X. Zheng, F. Wang, C. Y. Yam, Y. Mo, and G. H. Chen, Phys. Rev. B **75**, 195127 (2007).
[15]C. Yam, Y. Mo, F. Wang, X. Li, G. H. Chen, X. Zheng, Y. Matsuda, J. Tahir-Kheli, and W. A. Goddard III, Nanotechnology **19**, 495203 (2008).
[16]J. S. Ayubi-Moak, S. M. Goodnick, S. J. Aboud, M. Saraniti, and S. El-Ghazaly, J. Comput. Electron. **2**, 183–190 (2003).
[17]J. S. Ayubi-Moak, S. M. Goodnick, and M. Saraniti, J. Comput. Electron. **5**, 415–418 (2006).
[18]K. J. Willis, J. S. Ayubi-Moak, S. C. Hagness, and I. Knezevic, J. Comput. Electron. **8**, 153–171 (2009).
[19]K. J. Willis, S. C. Hagness, and I. Knezevic, Appl. Phys. Lett. **96**, 062106 (2010).
[20]R. O. Grondin, S. M. El-Ghazaly, and S. Goodnick, IEEE Trans. Microwave Theory Tech. **47**, 817–829 (1999).
[21]R. Eymard, T. Gallouet, and R. Herbin, "Finite volume methods," in *Handbook of Numerical Analysis* (Elsevier, Holland, 2000).
[22]P. Meuris, W. Schoenmaker, and W. Magnus, IEEE Trans. Comput.-Aided Des. **20**, 753–762 (2001).
[23]W. Schoenmaker and P. Meuris, IEEE Trans. Comput.-Aided Des. **21**, 534–543 (2002).
[24]Magwel, see http://www.magwel.com/ for more details about the commercial software MAGWEL.

[25] W. C. Chew, M. S. Tong, and B. Hu, *Integral Equation Methods for Electromagnetic and Elastic Waves* (Morgan & Claypool, 2009).

[26] D. J. Griggiths, *Introduction to Electrodynamics* (Prentice-Hall, New Jersey, 1999).

[27] A. Taflove and S. C. Hagness, *Computational Electrodynamics: The Finite-Difference Time-Domain Method*, 3rd ed. (Artech House, 2005).

[28] J. Yuen-Zhou, D. G. Tempel, C. A. Rodríguez-Rosario, and A. Aspuru-Guzik, Phys. Rev. Lett. **104**, 043001 (2010).

[29] B. Wang, Y. Xing, L. Zhang, and J. Wang, Phys. Rev. B **81**, 121103 (2010).

[30] M. Di-Ventra and R. D'Agosta, Phys. Rev. Lett. **98**, 226403 (2007).

[31] H. Xie, F. Jiang, H. Tian, X. Zheng, Y. Kwok, S. Chen, C. Yam, Y. Yan, and G. H. Chen, J. Chem. Phys. **137**, 044113 (2012).

[32] L. P. Kadanoff and G. Baym, *Quantum Statistical Mechanics: Green's Function Methods in Equilibrium and Nonequilibrium Problems* (Addison-Wesley, 1989).

[33] Y. Mo, X. Zheng, G. H. Chen, and Y. Yan, J. Phys.: Condens. Matter **21**, 355301 (2009).

[34] M. P. Anantram and S. Datta, Phys. Rev. B **51**, 7632–7639 (1995).

[35] B. Wang, J. Wang, and H. Guo, Phys. Rev. Lett. **82**, 398–401 (1999).

[36] Y. Wei and J. Wang, Phys. Rev. B **79**, 195315 (2009).

[37] C. G. Broyden, Math. Comput. **19**, 577–593 (1965).

[38] M. Elstner, D. Porezag, G. Jungnickel, J. Elsner, M. Haugk, T. Frauenheim, S. Suhai, and G. Seifert, Phys. Rev. B **58**, 7260–7268 (1998).